

# 3D MODELING OF EARTHQUAKE CYCLES OF THE XIANSHUIHE FAULT, SOUTHWESTERN CHINA

Li Xiaofan\*  
MEE09177

Supervisor: Bunichiro Shibazaki \*\*

## ABSTRACT

We perform 3D modeling of earthquake generation of the Xianshuihe fault, southwestern China, which is a highly active strike-slip fault with a length of about 350 km, in order to understand earthquake cycles and segmentations for a long-term forecasting and earthquake nucleation process for a short-term forecasting. Historical earthquake data over the last 300 years indicates repeated periods of seismic activity, and migration of large earthquake along the fault during active seismic periods. To develop the 3-D model of earthquake cycles along the Xianshuihe fault, we use a rate- and state-dependent friction law. After analyzing the result, we find that the earthquakes occur in the reoccurrence intervals of 400-500 years. The earthquake firstly occurs in the middle part of the fault in the year of 372. Then the second earthquake in the year of 858 occurs only along the main part of the fault but not the 0-100km part. After two earthquake cycles, the fault has been divided into 3 segments, which means since the third earthquake cycle, earthquake ruptures only occur in some parts of the fault, but not the whole fault line. This may be caused by the shape of the fault which has some bending parts. After comparison of the slip velocity at different depths, we find that the largest slip velocity occurs at the depth of 10km which is the exact depth of the seismic zone where fast rupture occurs.

**Keywords:** the Xianshuihe Fault, Earthquake Cycle, Rate- and State-dependent Friction Law, 3D Modeling.

## 1. INTRODUCTION

The Xianshuihe fault is located along the eastern margin area of the Tibetan plateau, southwestern China (Kato et al. 2007). There is a larger-scale fault system which is combined by the Ganzi-Yushu fault, the Xianshuihe fault, the Anninghe fault, the Zemuhe fault and the Xiaojiang fault from northwest to southeast and the slip motion releases strain that is related to collision of the Indian and Eurasian plates. As a part of this fault system, the Xianshuihe fault is a highly active strike-slip fault with the length of about 350 km.

The data that can be used to study earthquake recurrence are quite limited because recurrence times are generally large – a hundred years or more. As to Xianshuihe fault, we have very accurate earthquake catalogue since 1700. Historical earthquake data over the last 300 years indicates repeated periods of seismic activity, and migration of large earthquake along the fault during active seismic periods. 8 earthquakes of  $M_s \geq 7$  and 22 earthquakes of  $M_s \geq 6$  had occurred along the fault since 1700, among which Kangding  $M_s=7.8$  Earthquake was the biggest one. During recent 50 years (1923-1973), 3 earthquakes of  $M_s \geq 7.3$  had occurred along the Xianshuihe fault.

Figure 1 indicates the space-time distribution of  $M_s \geq 6.8$  earthquakes along the 4 main segments of the Xianshuihe fault.

---

\* Assistant researcher, China Earthquake Network Center, Beijing, China.

\*\* Researcher, International Institute of Seismology and Earthquake Engineering, Tsukuba, Japan.

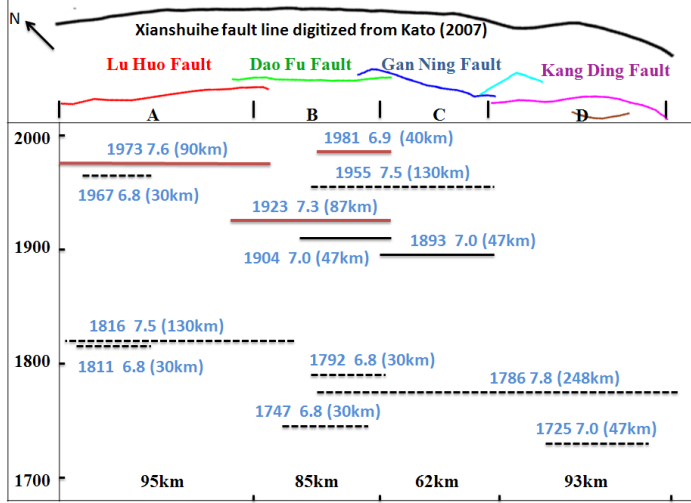


Figure 1. Space-time distribution of  $M_s \geq 6.8$  earthquakes along the 4 segments of the Xianshuihe fault. The black fault line is digitized from Kato et al. (2007) and the colored one is determined by geological survey by Deng et al. (1976). The blue roman numbers indicate the year in which earthquakes occurred, the earthquake magnitude ( $M_s$ ) and the numbers in parenthesis mean the length of rupture zones. Red and solid lines show certain and possible rupture zones, respectively. In the case of the dotted lines, we know time, magnitude and the fault zone in which the earthquake occurred. The lengths are determined by the scaling law by Fujii and Matsu'ura (2000).

According to this figure, we find that most of the earthquake ruptures only occurred along one segment or within one segment, while there were some large earthquakes ruptured across two segments of the fault. Therefore, these segments are somehow independent to each other and also have relations among them.

We need to understand earthquake cycles and segmentations for a long-term forecasting, and earthquake nucleation process for a short-term forecasting. Purpose of this study is to develop a 3-D model and then we can investigate the nucleation and earthquake cycles along the Xianshuihe fault. Model developed by Kato et al. (2007) is a 2-D model and they do not consider the fault slip variation with depth. However, the fault zone consists of the unstable and deeper stable zone. Therefore it is necessary to develop a 3-D model.

## 2. MODELING PROCEDURES

To develop a model of earthquake generation processes, firstly, we need to build a 3D mesh which represents the fault surface. And then, we have to consider a fault constitutive law which represents a physical property of the fault zone. Next it is necessary to consider a tectonic loading process in which stress is accumulated by the delay of the fault slip from the average slip rate of the fault zone. After that, we use the Runge-Kutta method with an adaptive step size control to gain the output of slip velocity and stress. Compared with observation, it is necessary to change some parameters to approach the observed historical data.

### 2.1 Basic equations

#### 2.1.1 Rate-and state-dependent friction

Since earthquakes can be regarded as a fault slip on the fault zone, a frictional constitutive law is important for understanding of earthquake generation processes. One representative friction law is rate- and state- dependent friction law, introduced by Dieterich (1981) and Ruina (1983).

The Dieterich/Ruina friction law with cut-off velocities proposed by Okubo (1989) is used to represent the frictional behavior that exhibits velocity weakening at low slip velocity and velocity strengthening at high slip velocity. Frictional resistance  $\tau$  depends on both slip velocity rate and state:

$$\tau = \mu \sigma_n^{eff} = \mu(\sigma_n - P_f) \quad (1)$$

$$\mu = \mu_* - a \ln\left(\frac{v_1}{v} + 1\right) + b \ln\left(\frac{v_2^\Theta}{D_c} + 1\right) \quad (2)$$

$$\frac{d\Theta}{dt} = 1 - \frac{\Theta v}{D_c} \quad (3)$$

where  $\mu$  is the coefficient of friction;  $\mu_*$ ,  $a$  and  $b$  are experimentally determined constants;  $\sigma_n^{eff}$  is the effective normal stress;  $\sigma_n$  is the lithostatic pressure;  $P_f$  is the pore pressure;  $v$  is the instantaneous sliding velocity,  $v_1$  is the cut-off velocity to a direct effect,  $\Theta$  is a state variable that characterizes the evolving state of the sliding surfaces both the slip- and normal stress- history; and  $v_2$  is the cut-off velocity to an evolution effect. Further,  $D_c$  is a critical displacement scaling for the evolution of the state variable. The state variable  $\Theta$  has the dimensions of time and interpreted to be a measure of the age of the population load-supporting contacts, which evolve with contact time, slip and the changes of normal stress (Dieterich, 2009).

From the equation, we can notice that steady state friction decreases with increasing slip velocity when  $a-b < 0$  and increases with increasing slip velocity when  $a-b > 0$ . If  $a-b < 0$ , this case is called velocity weakening, and it corresponds to the seismogenic zone, where stick and slip occur. On the other hand, if  $a-b > 0$ , the slip is stable, which is called velocity strengthening.

### 2.1.2 Loading processes

The shear stress  $\tau_{i,j}$  on the  $ij$ -cell on the fault is accumulated by the delay of the fault slip  $u_{i,j}$  from long-term fault slip, so that

$$\tau_{i,j} = \sum_{i_s, j_s} k_{i-i_s, j-j_s} (V_{pl}t - u_{i_s, j_s}) - \frac{G}{2\beta} \frac{du_{i,j}}{dt} \quad (4)$$

where  $\tau_{i,j}$ ,  $u_{i,j}$  and  $V_{pl}$  are the shear stress, the left-lateral slip at the  $ij$ -cell and the long-term tectonic slip rate at the  $ij$ -cell, respectively;  $G$  is the shear modulus and  $\beta$  is shear wave velocity;  $k_{i-i_s, j-j_s}$  is the elastostatic kernel that is the stress at the center of the  $ij$ -cell caused by uniform slip over the  $i_s, j_s$ -cell. The first term in the equation represents the tectonics loading due to relative plate motion. Since  $k_{i-i_s, j-j_s}$  does not include dynamic stress changes, the second term is necessary to represent the dumping factor for energy radiation through seismic waves introduced by Rice (1993).

By solving the coupled constitutive equations (1)-(3) and the equation of tectonics loading (4) using the Runge-Kutta method (Press et. al., 1992), the slip velocity and shear stress histories can be obtained.

## 2.2 Model Geometry and Discretization

The Xianshuihe fault is simply modeled by a curved fault surface in a three dimensional homogeneous isotropic elastic half space. The fault line is taken from Kato et. al., (2007). We build a model of earthquakes generation cycles on a curved surface of  $347\text{km} \times 24\text{km}$ , which represents the Xianshuihe fault surface. In this model, depth variation in frictional properties is included. To represent the slip velocity distribution on the fault surface, it is discretized into subfaults, each of which is  $0.8\text{ km}$  by  $0.8\text{ km}$  in the  $x$  and the  $y$  directions as shown in Figure 2. The slip velocity and the state variable are uniform on each subfault.

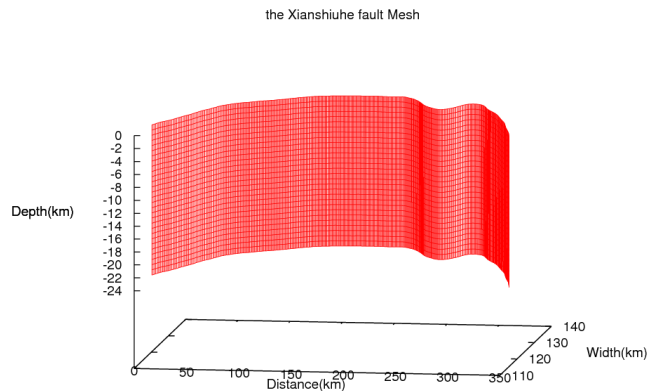


Figure 2. Meshes for 3-D model of the Xianshuihe Fault Surface

## 2.3 Distribution of frictional properties

Frictional properties control whether stick-slips or stable slidings occur on the fault. Frictional properties change with temperature based on laboratory experiments. Since temperature distribution on the plate boundary has not been known yet, we simply assumed that frictional parameters basically depend on depth (Hori, 2006). The depth distribution of the frictional parameters  $a$ ,  $b$  and  $D_c$  is shown in Figure 3. In horizontal direction there are no variations in friction parameters. The region where  $a-b$  is negative corresponds to the seismogenic zone, where stick and slip occur.

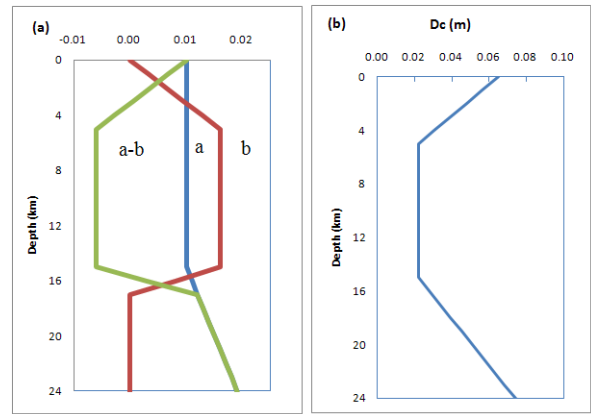


Figure 3. (a) The depth dependence of  $a$ ,  $b$  and  $a-b$ . (b) The depth dependence of the critical displacement  $D_c$ .

## 3. SIMULATION RESULTS

We simulate several earthquake cycles until around 2700 years. Identical earthquake occurs repeatedly with almost constant recurrence interval (400-500 years).

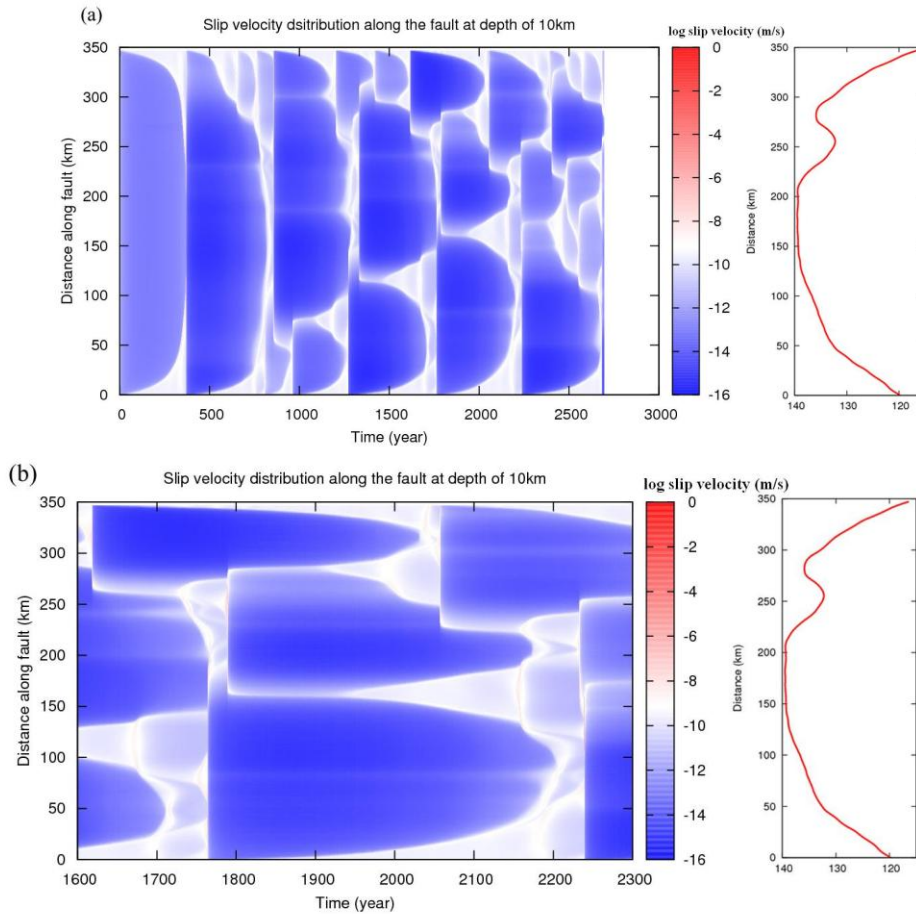


Figure 4. (a) Slip velocity distribution along the Xianshuihe fault at depth of 10km. Blue and red colored areas show the low and high velocity areas. The red line on the right is the fault line according to the distance along the fault. (b) Slip velocity distribution along the Xianshuihe fault at depth of 10km from the year of 1600 to 2300.

Figure 4a shows calculated slip velocity distribution along the fault at the depth of 10km during 2694 years along the Xianshuihe fault. Low and high velocity areas (blue and red colored areas in Figure 4) can be regarded as stick and seismic slip areas, respectively. In the interseismic period, most of the seismogenic zone is stick and stress is accumulated. After comparison of the slip velocity at different depths, we find that the largest slip velocity occurs at the depth of 10km. This depth is the exact depth of the seismic zone where fast rupture occurs.

According to this slip velocity distribution, we can find the fault line has been divided into 3 segments, which means since the third earthquake cycle, earthquake ruptures only occur in some parts of the fault, but not the whole fault line. That may be caused by the shape of the fault which has some bending parts, and somehow it is similar to the reality that the Xianshuihe fault is divided mainly into 4 segments.

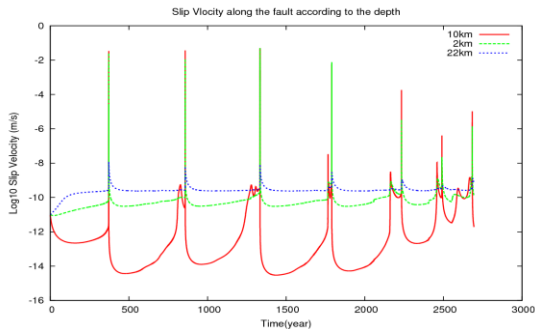


Figure 5. Slip velocity along the fault at different depths from shallow to deep.

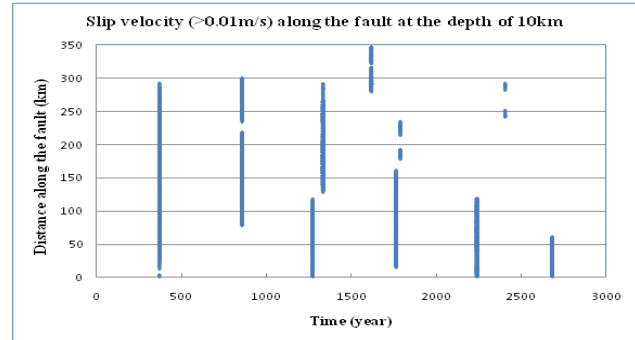


Figure 6. Slip velocity  $> 0.01\text{m/s}$  distributions along the fault.

Figure 5 shows the slip velocity of 3 cells at different depths from shallow to deep, 2km, 10km and 22km, respectively. It is easy to see that larger slip velocity occur at the depth of 10km, and the slip velocity becomes smaller while the depth increases and decreases. From Figure 6, we can know where ruptures occur and how ruptures migrate. In this study, the largest velocity is  $0.55\text{m/s}$ , which is close to the coseismic slip velocity  $1\text{m/s}$ . We check the cells of which slip velocity is larger than  $0.01\text{m/sec}$  and we can find that the earthquakes occur in the year of 372, 858, 1273, 1764, 2239 and 2684. The occurrence time is 400-500 years which is larger than the value of historical earthquake catalogue. The reason of this difference may be caused by the friction parameters that we used in this study.

#### 4. DISCUSSION AND CONCLUSIONS

We need to understand earthquake cycles and segmentation for a long-term forecasting and earthquake nucleation process for a short-forecasting. In the study herein, we perform a numerical simulation of seismic activity along the Xianshuihe fault, assuming that the long-term slip rates are consistent with geologically- and geodetically-derived values, and the friction on the fault obeys a rate- and state-dependent friction law. We investigate the nucleation and cycles of earthquakes along the Xianshuihe fault by a 3-D model. A large number of simulations have been run, and best result has been chosen to report.

According to Figure 6 showing the location of the slip velocity greater than  $0.01\text{m/s}$ , we can find that the earthquakes occur in the year of 372, 858, 1273, 1764, 2239 and 2684; the occurrence interval is 400-500 years. The earthquake firstly occurs in the middle part of the fault in year of 372, and then some obvious changes of the slip velocity can be found on the edges of both sides of the fault. In the year of 858, the second earthquake occurs along the mainly part of the fault except the 0-100km part of the fault. After two earthquake cycles, we find that the fault has been divided into 3 parts.

The recurrence interval of each earthquake depends both on a-b and Dc. So we should choose appropriate values of them to get close to the historical earthquake catalogue. If a large Dc value is chosen, slip instability becomes weak and no large seismic slip can occur. Whether a rupture stops or not also depends on the distribution of a-b and Dc values. Their spatial pattern and the values of a-b are determined based on other observational or experimental information. Additional examination is necessary to check if the Dc value used here is reasonable or not.

As we explained above, the fault line used for building the fault mesh is digitized from Kato et al., (2007). For simplicity, they combined the Xianshuihe fault into one main fault with two small ones. For this study, we just take the main fault into consideration. Actually, the Xianshuihe fault is divided into 4 main segments and 2 sub-segments, and the relation between them is complicated. It's better for us to develop a model with several segments to simulate.

The observed coseismic slip velocity is around 1m/s, and in our study, the largest slip velocity is 0.55m/s which is close to the coseismic slip velocity. The occurrence interval of earthquakes in this study is 400-500 years and the occurrence interval of the historical earthquakes is less than 200 years. Although we have already changed the parameters of 7 cases, we can not get the ideal results. Therefore, we may have to continue making some changes to the values of the frictional law parameters or changes to the mesh of fault to get better results.

## ACKNOWLEDGEMENT

We used the computer systems at the Earthquake Information Center of the Earthquake Research Institute, University of Tokyo, Tokyo, Japan.

## REFERENCES

- Deng Q. D., Zhang Y. M., Huan W. L. et. al., 1976, Chinese active faults and earthquake epicenter distribution map (1:3000000), China Earthquake Administration.
- Dieterich, J. H., 1981, Constitutive properties of rock with simulated gouge, in mechanical behavior of crustal rocks, *Geophys. Monogr. Ser.*, vol. 24, edited by N. L. Carter et al., pp. 108-120, AGU, Washington, D. C.
- Dieterich, J. H., 2009, Applications of rate- and state- dependent friction to models of fault slip and earthquake occurrence, *Earthquake Seismology*, 4, 107-129, Elsevier B.V., Netherlands.
- Fujii, Y., and Matsu'ura, M., 2000, Regional difference in scaling laws for large earthquakes and its tectonic implication, *Pure Appl. Geophys.*, 157, 2283-2302.
- Hori, T., 2006, Mechanisms of separation of rupture area and variation in time interval and size of great earthquakes along the Nankai Trough, southwest Japan, *Journal of the Earth Simulator*, 5, 8-19.
- Kato, N., Lei, X. L., and Wen, X.Z., 2007, A synthetic seismicity model for the Xianshuihe fault, southwestern China: simulation using a rate- and state-dependent friction law, *Geophys. J. Int.* 169, 286–300, doi:10.1111/j.1365-246X.2006.03313.x.
- Okubo, P.G., 1989, Dynamic rupture modeling with laboratory-derived constitutive relations, *J. Geophys. Res.*, 94(B9), 12,321-12,335, doi:10.1029/JB094iB09p12321.
- Press, W. H., Teukolsky, S. A., Vetterling, W.T., and Flannery, B.P., 1992, Numerical recipes in Fortran77, 707-752, Cambridge Univ. Press, New York.
- Rice, J. R., 1993, Spatio-temporal complexity of slip on a fault, *J. Geophys. Res.*, 98(B6), 9885-9907, doi:10.1029/93JB00191.
- Ruina, A., 1983, Slip instability and state variable friction laws, *J. Geophys. Res.*, 88(B12), 10,359-10,370, doi:10.1029/JB088iB12p10359.